

https://doi.org/10.1070/QEL18027

Absorption spectra and mechanical properties of C:F nanocoatings deposited from laser plasma onto leucosapphire surface

P.B. Sergeev, K.S. Kravchuk, N.V. Morozov

Abstract. **It is experimentally shown that during laser annealing of micron layers of fluorocarbon oil by high-power KrF laser radiation pulses, C:F nanocoatings with a thickness of up to ~100 nm can be synthesised on a leucosapphire surface. The absorption spectra of these coatings, measured in the 0.19–6 μm range, virtually coincided with the absorption spectra of fluorographene in the quantum energy range of 5 ± 1 eV. The nanohardness and elasticity modulus of the C:F nanocoatings are found to be 7 and 250 GPa, respectively, which is close to the characteristics of fluorographene.**

Keywords: *C:F nanocoating, absorption spectrum, laser plasma, KrF laser, leucosapphire, fluorocarbon oil.*

1. Introduction

A unique set of properties of fluorographene (FG) was presented in [1]. Compared to graphene, FG is an insulator. This is the thinnest insulating film, which also has a very high thermal and chemical resistance. The Young's modulus of FG is 300 GPa, which is only three times less than that of graphene. This value determines the ultimate strength characteristics of solid-state fluorocarbon (C:F) materials. It should be noted that currently widely used materials of this family are fluoroplastics of the Russian F-4 type [2]. Their Young's modulus is almost 1000 times smaller than that of FG [2]. Various strength characteristics of carbon structures [3, 4] and the developed methods for their fluorination [2, 5] indicate the possibility of developing fluorocarbon materials with strength parameters significantly exceeding fluoroplastic ones. To implement this, the development of appropriate technologies is required.

The possibility of deposition of C:F nanofilms on a titanium surface, formed from laser plasma during annealing of a thin layer of fluorocarbon oil (FO) by high-power KrF laser radiation, was shown in [6]. The resulting nanocoatings up to 60 nm thick had the Young's modulus of 130 GPa, which is only three times less than that of FG, but 300 times greater than that of fluoroplastic. Such unique strength characteristics require a more detailed study of these very promising nanocoatings and the determination of conditions for their synthesis. First of all, it is necessary to clarify the role of the titanium substrate, since a strong Ti–C bond can result in a high strength of C:F nanocoatings. Obviously, to do this, it is necessary to synthesise similar films on the surfaces of other materials and compare their characteristics.

The aim of this work was to examine the possibility of synthesising high-strength C:F nanocoatings on the surface of leucosapphire from laser plasma formed by the action of high-power KrF laser radiation on thin FO layers. The choice of the Al_2O_3 crystal for the planned experiments was dictated by studying not only the strength, but also the optical properties of the synthesised nanocoatings, which is much easier to perform on transparent substrates. In addition, it was supposed to verify the conclusions [7] about the resistance of Al_2O_3 samples to shock loads arising from the formation of laser plasma on their surface.

2. Methods for the synthesis and investigation of C:F nanocoatings on leucosapphire

An electron-beam KrF laser of the ELA facility [8] was used in experiments, which allows laser radiation (LR) pulses to be generated at a wavelength of 248 nm with an energy of up to 10 J and a duration of about 80 ns. The LR energy was controlled in each pulse. In these experiments, LR focusing provided uniform illumination of a spot with a diameter of 9 mm. The maximum LR energy density (fluence F) in such a spot reached 10 J cm^{-2}, while the intensity was 120 MW cm^{-2}. All other details of the experiments remained the same as in [6, 7]. In particular, thin (from ~1 to 10 μm thick) layers of the same FO were applied to the surface of leucosapphire plates as a coating material [6].

The plates of Al_2O_3 with a thickness of 3 mm were cut from a single crystal in the form of a square with a side of 15 mm. The polished working faces of the plates had the fourth grade of cleanness at a roughness $R_a \sim 0.010$ μm. The choice of the geometry and material of the plates was due to the requirement for their maximum strength under shock loads with an amplitude of ~10^8 Pa, which occur during the formation of laser plasma on the surface at LR intensities of ~100 MW cm^{-2} [7]. The size of the Al_2O_3 plates made it possible to fit on them up to four laser-irradiated spots with a diameter of 9 mm. On each plate, the place of one of the spots was reserved for recording with spectrophotometers of their 'zero' transmittance T_0, which was then used in calculating the transmittance of coatings synthesised on this plate.

The spectral study of clean Al_2O_3 substrates and all substrates with C:F nanocoatings was conducted using three spectrophotometers: Hitachi U-3900 (spectral range 0.19–

P.B. Sergeev, N.V. Morozov Lebedev Physical Institute, Russian Academy of Sciences, Leninsky prosp. 53, 119991 Moscow, Russia; e-mail: sergeevpb@lebedev.ru;
K.S. Kravchuk Technological Institute of Superhard and Novel Carbon Materials, ul. Tsentral'naya 7a, 108840 Moscow, Troitsk, Russia

Received 20 October 2021
Kvantovaya Elektronika **52** (4) 376–381 (2022)
Translated by M.A. Monastyrskiy

1.1 μm), Cary 5000 (0.8–3.3 μm), and FSM 2201 Fourier spectrometer (1.3–6 μm). Transmission spectra $T(\lambda)$ were recorded by all instruments in digital format with a wavelength step λ of no more than 1 nm. In this case, there was a significant overlap of the edge sections of the spectra recorded by different spectrophotometers. This circumstance was used to combine and stitch individual sections of the spectrum into a common one. The points of such stitching were close to 1 and 3 μm.

Measurements of the transmittance T_0 of a large number of Al_2O_3 plates showed that the averaged value of T_0 for them at a wavelength of 248 nm is 70.7 % ± 0.9 %, while in the range from 0.7 to 4 μm it amounts to 86 % ± 0.5 %. Variations in T_0 are due to both instrumental errors and random distribution of defects in the structure and surface of the plates. In experiments, when laser radiation was supplied to the FO layer through leucosapphire plates, their transmission was measured directly using LR. The obtained values of T_0 were used to calculate F on the output surface. In this case, the nonlinearities of KrF laser radiation absorption in Al_2O_3 plates [9, 10] were automatically taken into account.

The first experiments to test the possibilities of synthesising C:F nanofilms on leucosapphire by annealing layers of pure FO with a thickness of 1 to 10 μm were carried out according to the scheme of LR supply through the substrate. In this case, the maximum reduction in the transmission T of spots irradiated with high LR fluences did not exceed 10 %, which did not greatly exceed the measurement error. It was possible to almost double this value, and, consequently, increase the thickness of the synthesised coatings, by laser annealing of the FO layers on the front faces of the substrates. The maximum change in transmission in the samples tested according to this scheme was detected in a spot irradiated with two LR pulses at F = 6.8 and 6.3 J cm^{-2}. In this case, before the second pulse, oil residues from nonirradiated areas were smeared over the laser spot area, and the oil layer thickness was about 1 μm. Before the first laser shot, the FO layer had a thickness of about 10 μm. The corresponding spectra from this region, as well as other characteristics, will be indicated below by number 1.

In order to clarify the possible effect of titanium on the properties of synthesised C:F nanocoatings, as well as to increase the LR absorption, in the second series of experiments, instead of a layer of pure FO, an FO layer with the addition of TiC powder was deposited on the front faces of leucosapphire substrates. The particle size of the powder was about 1.2 μm, and its mass content in FO was ~1/10. In this case, the greatest changes in the transmission spectra were observed for the sample irradiated by four LR pulses at F = 8.1, 7.8, 8, and 7.3 J cm^{-2}. Here, the thicknesses of the FO layers for each subsequent pair of pulses alternated from 10 to ~1 μm. All the characteristics of this sample are indicated below by number 2. Note that the differences in $T(\lambda)$ for the samples irradiated by two and four LR pulses with close fluences did not exceed 20 % in both the first and second series of experiments.

To find out the possible effect of titanium foil on the properties of the deposited C:F nanofilms, we used another arrangement of irradiated materials. A layer of FO was deposited on the output face of a leucosapphire substrate, and a titanium foil with a thickness of 14 μm was applied to the layer. The foil was pressed against the substrate with adhesive tape. The FO layer's thickness here was determined by the roughness of the substrate and foil and amounted to about 2 μm. In this scheme, KrF laser radiation was supplied to the FO layer on titanium through an Al_2O_3 substrate. As a result, C:F nanofilms were deposited from laser plasma simultaneously on the surface of titanium and on the surface of Al_2O_3. Since after the LR pulse, the titanium foil swelled at the irradiation site, only one laser 'shot' was fired in this scheme at each surface area. Number 3 in the figures denotes the results obtained for a spot on a leucosapphire surface irradiated with a fluence of F = 8.3 J cm^{-2}. In this case, the spectrum of $T(\lambda)$ differed as much as possible from the spectrum of $T_0(\lambda)$. It should be noted that with such an irradiation scheme, laser plasma is formed under conditions of strict restriction of expansion and additional LR absorption in titanium. As a result, the laser plasma parameters differ from those obtained by laser annealing of the FO layer only. The reasons for such differences were studied in work [11] and the literature cited therein. We will consider them when analysing the results obtained from the corresponding spectra.

The choice of the spectra of the listed samples for the analysis was due to the fact that, according to spectral measurements, the synthesised coatings on them had a maximum thickness. This was important in order to achieve maximum accuracy in subsequent measurements of the strength and structural characteristics of the resulting C:F nanocoatings. Such measurements were carried out using a nanohardness tester [NanoScan-4D, Technological Institute of Superhard and Novel Carbon Materials (TISNUM)] and a confocal optical profilometer (Sneox, Sensofar).

Figure 1a shows a 3D image of the surface relief of one of the sections of sample 2 in the region of the laser spot bound-

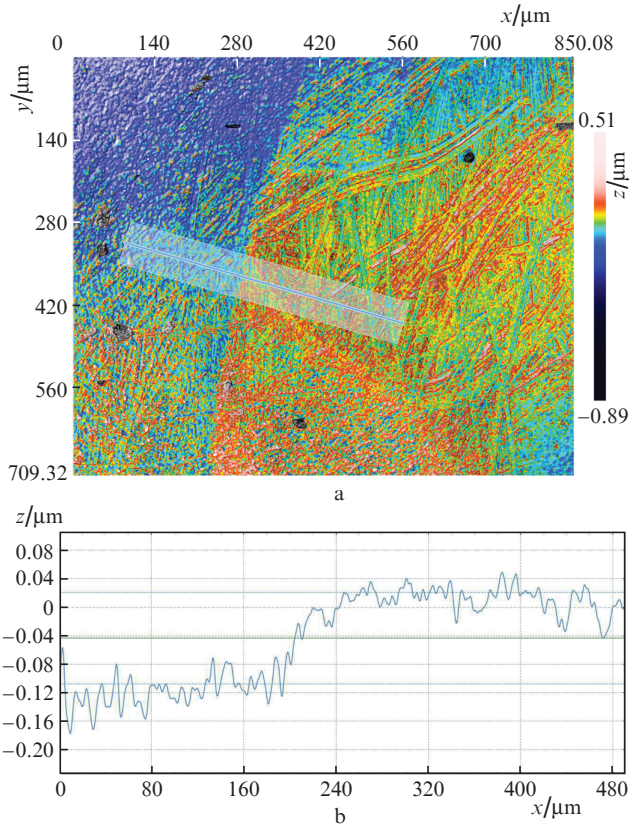

Figure 1. (Colour online) (a) 3D image of the surface relief at the boundary of the laser irradiation region of sample 2 and (b) the surface profile along the line highlighted in Fig. a.

ary, obtained with a profilometer. Figure 1b shows the surface profile along the line highlighted in Figure 1a with a grey rectangle. It can be seen that the roughness of the leucosapphire surface in sample 2 both in the laser spot area and beyond it is virtually the same. The parameter R_a in these regions is at the level of 8 and 7 nm, respectively. The profile jump can be used to estimate the C:F coating thickness, which in this region is about 100 nm.

3. Absorption spectra of C:F nanocoatings on leucosapphire

The transmission spectra of the corresponding three spots (1, 2, and 3) on leucosapphire samples are shown in Fig. 2a. A typical 'zero' transmission spectrum of one of the Al_2O_3 (0) plates is also shown here. This indicates that the region of absorption determination in the synthesised films from λ = 0.19 to 6 μm is limited by the transparency region of the leucosapphire plates. As can be seen from Fig. 2a, the spectra of samples 1 and 2 differ noticeably from the transmission spectrum of a clean plate only in the short-wavelength region with $\lambda < 1$ μm. The transmission of sample 3 is markedly lower than the original one in almost the entire recording range.

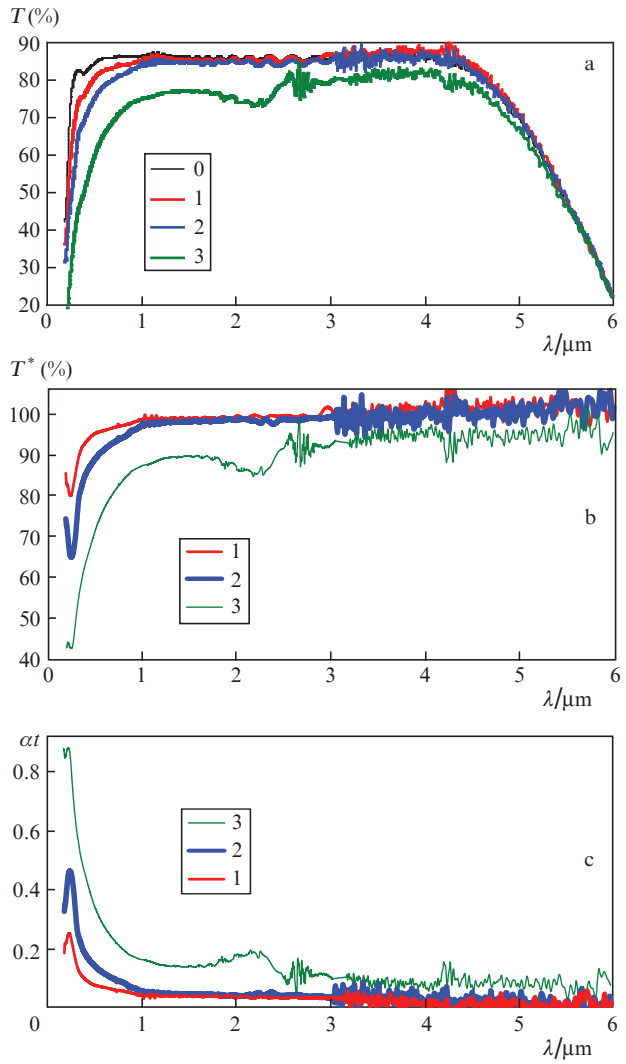

Figure 2. (Colour online) Transmission spectra of a clean sapphire leucosapphire plate (0) and samples 1, 2, and 3 (a), as well as calculated T_0-normalised transmission spectra of coatings on samples 1, 2, and 3 (b) and optical density spectra of coatings 1, 2, and 3 (c).

The reasons for such differences were revealed by comparing the surface reliefs of all samples. For samples 1 and 2, the surface roughness virtually did not differ from the initial value R_a = 6–8 nm. For sample 3, it increased by almost an order of magnitude, up to 50 nm. High peaks with an amplitude of up to 1 μm and wave-like structures with a width of up to 5 μm and a height of about 0.4 μm appeared. All this indicates the melting of the leucosapphire surface in this laser irradiation regime. Such modification of the Al_2O_3 surface leads to an increase in the scattering of radiation, the spectra of which can be qualitatively judged by the results of work [12]. It can also manifest itself in an increase in absorption on intrinsic and impurity defects [13–15], which appear in the molten and then rapidly cooled crystal layer. And all this happens in addition to the absorption on the deposited C:F coating. This complex multicomponent nature of the spectra of sample 3 must be borne in mind when comparing them with other spectra shown in Figs 2 and 3. The spectra of sample 3 should be considered as demonstration spectra for cases of FO laser annealing under extremely hard, with melting of the leucosapphire surface, laser irradiation.

To clarify the essence of the subsequent numerical manipulations with the original spectra displayed in Fig. 2a, we present several relations in which, for brevity, the components associated with interference effects are omitted. In this geometrical optics approximation, the transmission of a transparent plate of material A with a thickness t_A at a wavelength λ appears as

$$T_A = (1 - R_A)^2 \exp(-\alpha_A t_A). \quad (1)$$

Here R_A and α_A are the coefficient of reflection from the plate's face and the coefficient of its absorption, respectively. If the plate has a coating of material B with a thickness of t_B, then the transmission is

$$T_{AB} = (1 - R_A)\exp(-\alpha_A t_A)(1 - R_{AB})\exp(-\alpha_B t_B)(1 - R_B). \quad (2)$$

Here $R_{AB} = (n_A - n_B)^2/(n_A + n_B)^2$ is the coefficient of reflection from the boundary of materials A and B with refractive indices n_A and n_B; R_B and α_B are the reflection and absorption coefficients of the coating material B at a wavelength λ, respectively.

Relations (1) and (2) allow one to obtain the *calculated* transmission T_B^* of material B on the surface of material A:

$$T_B^* = (T_{AB}/T_A) = [(1 - R_{AB})(1 - R_B)/(1 - R_A)]\exp(-\alpha_B t_B). \quad (3)$$

It differs from the standard transmittance of layer B based on expression (1) (with the replacement of the subscript A by the subscript B with a different multiplier: instead of the factor $(1 - R_B)$, here we have $(1 - R_{AB})/(1 - R_A)$. This leads to the fact that in the region of low absorption, when $\exp(-\alpha_B t_B) \approx 1$, and $R_B < R_A$, the value of T_B^* can reach 100% or higher. In view of the above, let us turn to Fig. 2b which shows three normalised transmission spectra of synthesised C:F coatings calculated from the experimental results: $T_i^* = T_i/T_0$, where i = 1 – 3 are the numbers of the corresponding spots. It can be seen that for films from samples 1 and 2, a significant difference in transmission from 100% is only noticeable in the region $\lambda < 1$ μm, and for films from sample 3, over the entire recorded range.

Let us apply the standard definition of the optical density of a material layer, OD = ln(1/*T*), to T_i^*. Given that for small *R* values, ln(1 – *R*) ≈ (–*R*), we obtain

$$\mathrm{OD}_i^* = \ln(1/T_i^*) \approx \alpha_i t_i + R_{\mathrm{AB}} + R_{\mathrm{B}} - R_{\mathrm{A}}$$

or

$$\alpha_i t_i \approx \ln(1/T_i^*) + R_{\mathrm{A}} - R_{\mathrm{AB}} - R_{\mathrm{B}}. \quad (4)$$

For the leucosapphire plate (material A), $R_{\mathrm{A}} \approx 0.07$, and, according to estimates, $n_{\mathrm{B}} \sim 1.4$ for fluorocarbon films. Hence it follows that $R_{\mathrm{B}} \approx 0.03$, $R_{\mathrm{AB}} \approx 0.01$, and $R_{\mathrm{A}} - R_{\mathrm{AB}} - R_{\mathrm{B}} \approx 0.03$. This value was added to $\ln(1/T_i^*)$ when calculating, based on (4), the *physical* optical density $\alpha_i t_i$ of the films. The obtained spectra are shown in Fig. 2c. Given the transmission measurement errors, the accuracy of their determination is about 0.03. With this error, for coatings 1 and 2, $\alpha_i t_i \approx 0$ in the range from ~1.5 to 6 μm.

A common feature of all three spectra in Fig. 2c is the presence of a maximum at 250 nm (5 eV). To compare the spectra of all coatings in this region, we plotted the dependences of the normalised-to-maximum absorption coefficients $[\alpha_i t_i/(\alpha_i t_i)_{\max} = \alpha_i/\alpha_{i\ \max}]$ on the wavelength (Fig. 3a) and on the energy *E* of probing quanta (Fig. 3b). It turned out that the maxima of all spectra are in the narrow regions of wavelengths (245 ± 2 nm) and energies (5.1 ± 0.05 eV).

Spectra 1 and 2 in Fig. 3 are very similar to the absorption spectrum of fluorographene [1]. It also has a maximum at *E* = 5 eV and a half-width (on the side of lower energies from the maximum) of 1 eV. According to [16], this exciton absorption band is present in single-layer, two-layer, and multilayer fluorographene films. The similarity of the spectra of films 1 and 2 with fluorographene films near *E* = 5 eV shows for the first time that this band is also inherent in C:F nanofilms, which, according to [6], have an amorphous structure. The differences in the spectra of the materials under consideration are manifested in the variety of the wing shape of the exciton band, which is clearly seen in the spectra in Fig. 3.

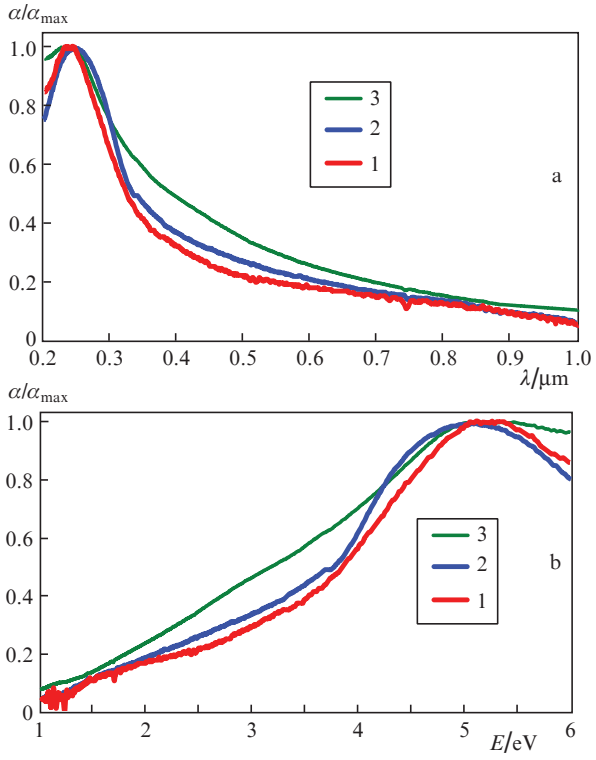

Figure 3. (Colour online) Absorption spectra of coatings 1, 2, 3, normalised to $\alpha_{\max}$, as functions of (a) wavelength and (b) energy of probing radiation quantum.

Visually, coatings 1 and 2 on the leucosapphire are almost invisible, while coating 3 has greyish colour. Consequently, the blackening of titanium samples, noted in [6] at the site of FO annealing by KrF laser radiation, is caused by a change in the colour of the titanium surface, and not by the colour of the C:F nanofilms covering it.

From the results of work [17] on the transmission of two multilayer fluorographene nanofilms, we can estimate their absorption coefficients at $\lambda = 0.4$ μm as 2.5×10^4 cm^{-1}. Using this value and the values of $\alpha_i t_i$ at the same wavelength as in Fig. 2c, we obtain estimates for film thicknesses as 1, 2, and 3: 40, 80, and 180 nm, respectively. Note that after FO annealing on titanium foil by four laser pulses, as in sample 2, the C:F coating thickness was 60 nm [6]. Measurements using a profilometer of the C:F-coating thickness at spot 3 near the melting zone from the clean surface side gave $t_3 \approx 160$ nm, while at spot 2, as can be seen from Fig. 1, $t_2 \approx 100$ nm. The totality of these results indicates the correctness of the assessment of the nanocoating thicknesses. The knowledge of *t* and the spectra of αt in Fig. 2c allow us to determine the maximum value of α at $\lambda = 245$ nm for the synthesised C:F nanocoatings, which amounted to $(6 \pm 2) \times 10^4$ cm^{-1}. This value and the spectra in Figs 2 and 3 provide an opportunity to identify fluorocarbon nanofilms and allow one to estimate their thicknesses from the absorption spectra in the UV region of the spectrum.

4. Mechanical properties of C:F nanocoatings on leucosapphire

Mechanical properties of the synthesised C:F nanocoatings were measured using a NanoScan-4D nanohardness tester at the TISNUM. This Russian device, mass-produced at the TISNUM, is included in the state register of measuring instruments. It is designed to determine the nanohardness and elasticity modulus of materials at depths up to ~1 μm. It implements the method of instrumental indentation of materials standardised in Russia (GOST R 8.748-2011), described in detail in many publications [18–20]. In NanoScan-4D, a standard diamond triangular Berkovich pyramid is used as an indenter; the maximum load on the indenter reaches 200 mN. Loading time at each point is 10 s. In the presented experiments, the number of sensing points for each load was about 15. As a result of the measurements, the dependences of the nanohardness *H* of the samples on the indenter immersion depth *h*, as well as similar dependences of the modulus of normal elasticity, were plotted. This value with an accuracy of 6% [21] coincides with the Young's modulus E_{Y}.

Figure 4a shows the dependences of *H*(*h*) obtained for the clean surface of leucosapphire samples (0) and three spots with C:F nanocoatings, as well as similar dependences for C:F nanofilms on titanium from [6]. The level of close measurement errors for all points in Fig. 4a is shown on the example of sample 1.

The nanohardness values of the coatings of samples 1 and 3 (one and two points in the range of minimum values of *h*) virtually coincide and amount to 7 ± 2.5 GPa. For sample 2,

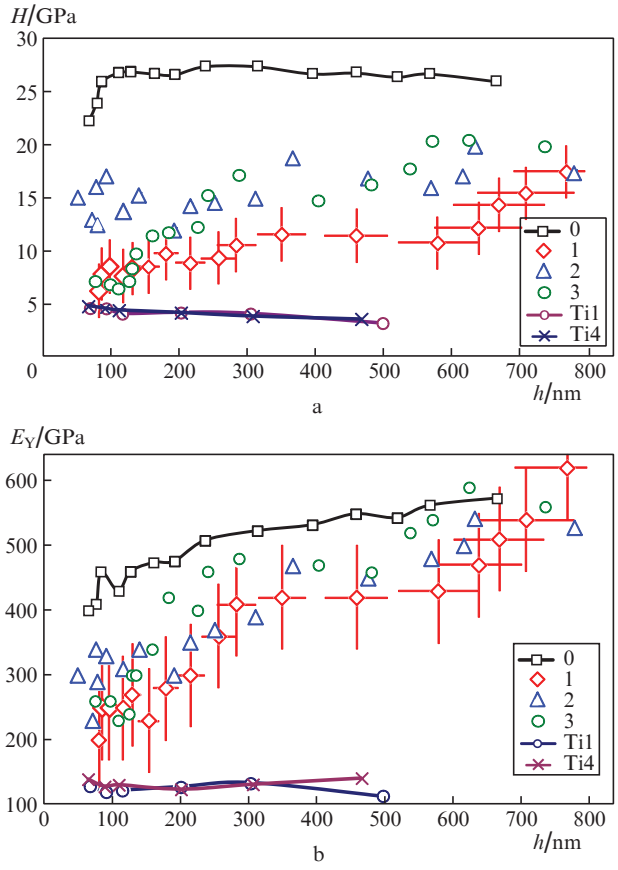

Figure 4. (Colour online) (a) Dependences of the nanohardness H on the indenter immersion depth h for the clean surface of leucosapphire samples (0) and samples 1, 2, and 3, as well as for the coatings on titanium (Ti1 and Ti4) from [6]; (b) dependences of the Young's modulus E_Y on h for the same samples.

the H value is approximately twice as large. Whether this is due to the presence of TiC powder in FO in this case remains an open question. For the same films on titanium, $H \approx 5$ GPa [6]. Similar hardness values of C:F nanocoatings on both titanium and leucosapphire are most likely a property of the coating material.

One more fact in Fig. 4 deserves attention. The hardness of the surface layer of all leucosapphire substrates after FO laser annealing noticeably, almost twice, decreases. Recall that the surface of the sample substrate 3 melts. The proximity of H values for the surface layers of all three samples indicates that, for samples 1 and 2, the surface heating during laser exposure was close to the melting temperature of leucosapphire, i.e. 2000 °C. And this heating, apparently, leads to cracking of the surface layer of leucosapphire samples to a depth of ~1 μm, which reduces their hardness.

It is also appropriate to note here that none of the leucosapphire plates cracked during the experiments described above at LR fluences up to 10 J cm^{-2}. In the third regime of FO laser annealing with titanium foil on the output surface of the samples, the pressure jump in the laser plasma due to the limitation of its expansion could reach ~10^9 Pa, which is an order of magnitude greater than that for the conditions implemented in [7]. This indicates a higher strength of leucosapphire samples compared to quartz samples in experiments on the synthesis of nanocoatings from laser plasma.

Figure 4b shows the dependences of the Young's modulus E_Y of samples on h, measured with a nanohardness tester. Almost the same level of measurement errors for all points is demonstrated by the example of sample 1. The values of E_Y for all three C:F nanocoatings on leucosapphire (points in the region $h < 100$ nm) are in the range of 250 ± 80 GPa. For similar nanocoatings on titanium $E_Y \approx 130$ GPa [6]. Thus, the synthesised C:F nanocoatings on both titanium and leucosapphire have an average value of $E_Y \approx 200$ GPa, which is comparable with the Young's modulus of 300 GPa for fluorographene [1].

5. Conclusions

We have experimentally proved the possibility of synthesising high-strength fluorocarbon nanocoatings on the surfaces of leucosapphire samples during annealing in air of a thin cover layer of fluorocarbon oil by radiation pulses from a high-power KrF laser. The absorption spectra of the synthesised C:F nanocoatings were measured, which are similar to the absorption spectra of fluorographene. The obtained spectral information makes it possible to identify C:F nanofilms and coatings and determine their thicknesses, which will greatly facilitate their further study.

The second important result of this work is the proof that the mechanical properties of the synthesised C:F nanocoatings on such different substrates as leucosapphire and titanium are similar. This allows us to argue that these properties are the properties of the nanocoating material, and their Young's modulus is comparable with that of fluorographene. If other unique physicochemical properties of fluorographene are also inherent in the synthesised material, questions about the scope of its application should not arise. However, there is still a lot of painstaking work to study the entire variety of properties of the obtained C:F nanocoatings, as well as the development of technologies for their use.

The work has experimentally confirmed the high strength of leucosapphire samples to shock loads arising from the generation of laser plasma on their surface with pressures up to ~10^9 Pa. It has been found that such impacts, accompanied by short-term heating of the near-surface layer of Al_2O_3 to temperatures of about 2000 °C, lead to an almost twofold decrease in the nanohardness of this layer. Perhaps this is due to its cracking.

Acknowledgements. The authors are grateful to their colleagues V.I. Kozlovsky and Ya.K. Skasyrsky for their help in carrying out spectral measurements.

References

1. Nair R.R., Ren W.C., Jalil R., Riaz I., Kravets V.G., Britnell L., Blake P., Schedin F., Mayorov A.S., Yuan S., Katsnelson M.I., Cheng H.M., Strupinski W., Bulusheva L.G., Okotrub A.V., Grigorieva I.V., Grigorenko A.N., Novoselov K.S., Geim A.K. *Small*, **6**, 2877 (2010); https://doi.org/10.1002/smll.201001555.
2. Panshin Yu.A., Malkevich S.G., Dunaevskaya Ts.S. *Ftoroplasty* (Fluoroplastics) (Leningrad: Chemistry, 1978) p. 232.
3. Robertson J. *Mater. Sci. Eng. R*, **37**, 129 (2002).
4. Spitsyn B.V., Aleksenko A.E. *Zashch. Met.*, **43**, 456 (2007).
5. Mitkin V.N. *J. Struct. Chem.*, **44** (1), 82 (2003) [*Zh. Strukt. Khim.*, **44** (1), 99 (2003)].
6. Sergeev P.B., Kirichenko A.N., Kravchuk K.S., Morozov N.V., Khmelnitsky R.A. *Quantum Electron.*, **50** (12), 1173 (2020) [*Kvantovaya Elektron.*, **50** (12), 1173 (2020)].

7. Sergeev P.B., Morozov N.V., Kirichenko A.N. *Quantum Electron*., **48** (2), 136 (2018) [*Kvantovaya Elektron*., **48**, 136 (2018)].
8. Sergeev P.B. *J. Sov. Laser Research*, **14** (4), 237 (1993); https://doi.org/10.1007/BF01120654.
9. Morozov N.V., Reuterov V.M., Sergeev P.B. *Quantum Electron*., **29** (11), 979 (1999) [*Kvantovaya Elektron*., **29** (2), 141 (1999)].
10. Barabanov V.S., Sergeev P.B. *Quantum Electron*., **25** (7), 717 (1995) [*Kvantovaya Elektron*., **22** (7), 745 (1995)].
11. Veiko V.P., Volkov S.A., Zakoldaev R.A., Sergeev M.M., Samokhvalov A.A., Kostyuk G.K., Milyaev K.A. *Quantum Electron*., **47** (9), 842 (2017) [*Kvantovaya Elektron*., **47** (9), 842 (2017)].
12. Yurina V.Yu., Neshchimenko V.V., Chundun Li. *Poverkhnost'. Rentgen., Sinkhrotron. Neitron. Issled*., (3), 46 (2020); doi: 10.31857/S1028096020030218; [*J. Synch. Investig.*, **14**, 253 (2020)]; https://doi.org/10.1134/S102745102002038X.
13. Vainshtein I.A., Kortov V.S. *Phys. Solid State*, **42** (7), 1259 (2000) [*Fiz. Tverd. Tela*, **42** (7), 1259 (2000)]; https://doi.org/10.1134/1.1131373.
14. Bityukov V.K., Petrov V.A. *Prikl. Fiz*., No. 4, 18 (2007).
15. Kortov V.S., Vainshtein I.A., Vokhmintsev A.S., Gavrilov N.V. *J. Appl. Spectrosc*., **75** (3), 452 (2008) [*Zh. Prikl. Spektrosk.*, **75** (3), 422 (2008)].
16. Karlicky F., Otyepka M. *Ann. Phys*., **526** (9–10), 408 (2014); https://doi.org/10.1002/andp.201400095.
17. Ivanov F.I., Nebogatikova N.A., Kotin I.A., Antonova I.V. *Phys. Chem. Chem. Phys*., **19**, 19010 (2017); doi: 10.1039/c7cp03609d.
18. Oliver W.C., Pharr G.M. *J. Mater. Res*., **7** (6), 1564 (1992).
19. Frolova M.G., Titov D.D., Lysenkov A.S., Kravchuk K.S., Istomina E.I., Istomin P.V., Kim K.A., Kargin Y.F. *Ceramics Intern.*, **46** (11), 18101 (2020); doi: 10.1016/j.ceramint.2020.04.130.
20. Golovin Yu.I. *Phys. Solid State*, **63** (1), 1 (2021) [*Fiz. Tverd. Tela*, **63** (1), 3 (2021)]; doi: https://doi.org/10.1134/S1063783421010108.
21. Chudoba T., Jennett N.M. *J. Phys. D: Appl. Phys*., **41** (21), 215407 (2008); doi: 10.1088/0022-3727/41/21/215407.